The Meteoritical Society

Meteoritics & Planetary Science 48, Nr 11, 2076–2089 (2013)
doi: 10.1111/maps.12091

Dawn completes its mission at 4 Vesta

C. T. RUSSELL[1*], C. A. RAYMOND[2], R. JAUMANN[3], H. Y. McSWEEN[4], M. C. De SANCTIS[5], A. NATHUES[6], T. H. PRETTYMAN[7], E. AMMANNITO[5], V. REDDY[6], F. PREUSKER[3], D. P. O'BRIEN[7], S. MARCHI[8], B. W. DENEVI[9], D. L. BUCZKOWSKI[9], C. M. PIETERS[10], T. B. McCORD[11], J.-Y. LI[12], D. W. MITTLEFEHLDT[13], J.-P. COMBE[11], D. A. WILLIAMS[14], H. HIESINGER[15], R. A. YINGST[7], C. A. POLANSKEY[2], and S. P. JOY[1]

[1]Institute of Geophysics and Planetary Physics, University of California, Los Angeles, 603 Charles Young Drive, 3845 Slichter Hall, Los Angeles, California 90096-1567, USA
[2]Jet Propulsion Laboratory, California Institute of Technology, MS 264-828, 4800 Oak Grove Drive, Pasadena, California 91109-8099, USA
[3]Deutsches Zentrum für Luft- und Raumfahrt (DLR), Institute of Planetary Research, Rutherfordstrasse 2, Berlin 12489, Germany
[4]Department of Earth and Planetary Sciences, University of Tennessee, 1412 Circle Drive, Knoxville, Tennessee 37996-1410, USA
[5]Istituto di Astrofisica e Planetologia Spaziali, Istituto Nazionale di Astrofisica, Via del Fosso del Cavaliere 100, 00133 Roma, Italy
[6]Max-Planck-Institut für Sonnensystemforschung, Max-Planck-Strasse 2, Katlenburg-Lindau, 37191, Germany
[7]Planetary Science Institute, 1700 E. Ft. Lowell Rd., Suite 106, Tucson, Arizona 85719, USA
[8]NASA Lunar Science Institute, Center for Lunar Origin and Evolution, 1050 Walnut Street, Suite 300, Boulder, Colorado 80302, USA
[9]Johns Hopkins University Applied Physics Laboratory, 11100 Johns Hopkins Rd, Laurel, Maryland 20723-6099, USA
[10]Department of Geological Sciences, Brown University, Box 1846, Providence, Rhode Island 02912, USA
[11]The Bear Fight Institute, P.O. Box 667, 22 Fiddler's Road, Winthrop, Washington 98862, USA
[12]Department of Astronomy, University of Maryland at College Park, CSS Bldg., Rm. 1204, Stadium Dr., College Park, Maryland 20742, USA
[13]NASA Johnson Space Center, Astromaterials Research Office, Mail code KR, NASA Johnson Space Center, 2101 NASA Parkway, Houston, Texas 77058, USA
[14]School of Earth and Space Exploration, Arizona State University, Bateman Physical Sciences F506B, Box 871404, Tempe, Arizona 85287-1404, USA
[15]Institut für Planetologie, Wilhelm-Klemm-Str. 10, 48149 Münster, Germany
[*]Corresponding author: E-mail: ctrussell@igpp.ucla.edu

(Received 04 September 2012; revision accepted 03 January 2013)

Abstract–The Dawn mission was designed to test our hypothesis about the origin and evolution of the early solar system by visiting the largest differentiated basaltic asteroid, 4 Vesta, believed to be a survivor from the earliest times of rocky body formation. Observations from orbit show that Vesta is the parent body of the Howardite, Eucrite, Diogenite meteorites. Vesta has an iron core and a eucritic–diogenitic crust. Its surface is characterized by abundant impact craters but with no evident volcanic features. It has two ancient impact basins in the southern hemisphere that are associated with circum-planetary troughs. The northern hemisphere is the more heavily cratered and contains the oldest terrains. The surface of Vesta is diverse, with north-south and east-west dichotomies in the eucrite-to-diogenite ratio. Its surface contains both very bright and very dark material, and its color varies strongly from region to region. Both the mineralogical and the elemental compositions agree with that expected for the HED parent body. Significant OH or H may be present in the upper crust and the presence of pits in "fresh" craters is consistent with the devolatilization of the surface after a collision either brought to or tapped a source of water on Vesta. The presence of dark material on the surface of Vesta suggests efficient transport pathways for organic material, and the mixing of the dark material with the more pristine pyroxene explains the varying albedo across the surface. Vesta has proven to be a reliable witness to the formation of the solar system.

INTRODUCTION

Dawn is the ninth mission in the Discovery program, a series of principal-investigator-led missions exploring the solar system. It is a unique scientific mission utilizing ion propulsion to leave the vicinity of the Earth and spiral outward to targets in the asteroid belt. When its heliocentric orbit matches that of its intended target, ion propulsion is used to slip into the body's gravitational potential well and descend until it reaches a desired mapping orbit. When it completes its mapping mission, it uses its ion thrusters to raise its orbital altitude and escape the body's gravity to achieve a heliospheric orbit around the Sun. The ion engine thrusts until reaching its next target, at which time it glides into orbit and begins mapping anew. Such a mission would be unaffordable using conventional technology, but through the power and economy of ion propulsion technology, Dawn is, in fact, the least expensive of the current Discovery missions.

Dawn's targets are 4 Vesta and 1 Ceres, the most massive asteroids in the Main Belt. These objects were chosen for study because they are intact witnesses to the events at the dawn of the solar system (hence the name of the mission). Vesta, in particular, underwent magmatic differentiation and began to solidify as early as about 2 Myr after the first condensation of solids in the solar nebula (McSween and Huss 2010). Ceres, however, is very different from Vesta. Its density tells us that it contains much water ice and possibly subsurface liquid water (McCord et al. 2011). This wetness may lead to a different style of differentiation and a more dynamic surface where endogenic processes destroy and renew the surface on short time scales compared with those of the evolution of the solar system.

It is not our purpose in this article to review either the earliest days of the solar system or the development of the Dawn mission. These stories are told in a special issue of *Space Science Reviews* that describes the history of Dawn's development (Russell and Raymond 2011), the flight system (Thomas et al. 2011), and the ion propulsion system (Brophy 2011). Included in this series of articles is a discussion of our current understanding of the history and evolution of the solar system (Coradini et al. 2011; O'Brien and Sykes 2011), as well as our expectations for the interiors and surfaces of Vesta (Pieters et al. 2011; Zuber et al. 2011) and Ceres (McCord et al. 2011; Rivkin et al. 2011). Rather, we review the results of the Vesta mapping that were available in the Fall of 2012. At the end of the article, we include a brief discussion of the observations at the north pole for which no papers have been published or presented at the time of this writing. We also discuss our measurement objectives and what measurements we did achieve.

A special feature of our exploration of Vesta is the existence of extensive geochemical investigations of the howardite, eucrite, and diogenite (HED) meteorites that have been associated with Vesta as their (ultimate) parent body. McCord et al. (1970) were the first to realize the implications of the reflectance spectrum of Vesta leading to the paradigm that Dawn was sent to test at Vesta. This paradigm was also later supported by strong geochemical evidence (Consolmagno and Drake 1977). The HED meteorites and the current understanding of their relationship to Vesta have been described by McSween et al. (2011). This understanding was used to develop a payload for the mission consisting of a framing camera (Sierks et al. 2011); a visible and infrared mapping spectrometer, dubbed VIR (De Sanctis et al. 2011); and a gamma ray and neutron spectrometer, called GRaND (Prettyman et al. 2011). These instruments were supplemented by the telemetry system that was used to obtain radiometric tracking data to define the gravitational field (Konopliv et al. 2011a). The framing camera was used to obtain observations of the surface from different viewing directions that were used to reconstruct the topography of the surface using stereophotogrammetry and stereophotoclinometry (Raymond et al. 2011; Jaumann et al. 2012; Preusker et al. 2012). Two other important aspects of the mission are the science planning, operations, and archiving processes described by Polanskey et al. (2011) and the education and public outreach programs (McFadden et al. 2011).

THE SPACECRAFT AND PAYLOAD

The spacecraft shown in Fig. 1 is three-axis stabilized with large solar arrays to provide the power to run the ion engines as well as operate the flight system and payload. To map the surface of Vesta and later Ceres, the spacecraft points its remote sensing instruments at the surface of the body. As it orbits, the spacecraft keeps its solar array pointed toward the Sun while its instruments are pointed at the surface. Data are recorded on the spacecraft for later transmission to the Earth. The spacecraft has to pause in its data taking and point its high-gain antenna to Earth for this data transfer.

The framing camera shown in Panel A of Fig. 2 comes as a redundant pair of which only one has been used thus far in accord with flight rules for redundant systems. It has a detector with 1024 by 1024 pixels and a filter wheel in the optical path with one clear and seven color filters. The cameras were provided by the Max Planck Institute for Solar System Research in

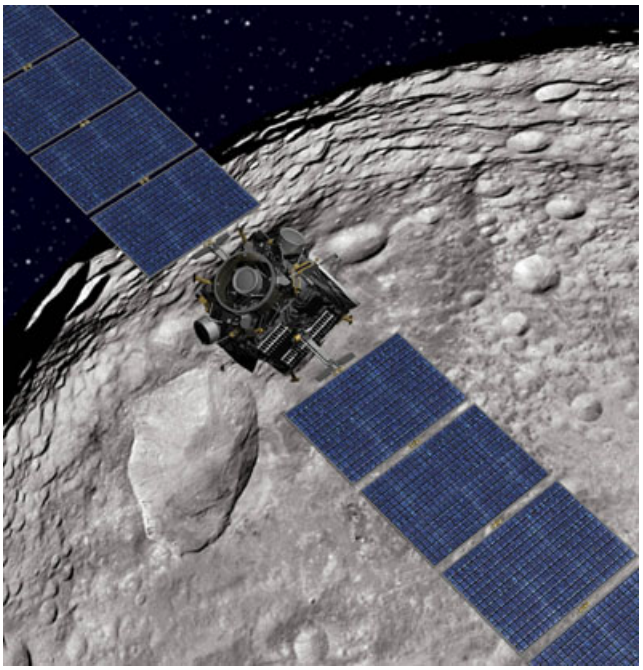

Fig. 1. Artist's concept of Dawn spacecraft orbiting Vesta. The instruments are on the unseen side of the spacecraft (nadir) pointing toward the surface. Visible are the three ion thrusters that are not used while the spacecraft is making scientific measurements. The solar array is pointed toward the Sun as Dawn moves across the sunlit surface of Vesta.

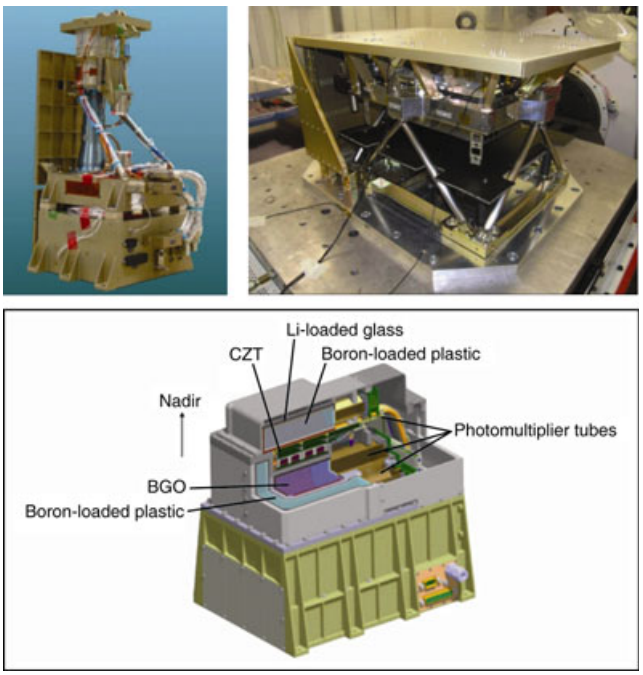

Fig. 2. (Upper left panel) The Framing Camera. (Upper right panel) The Visible and Infrared Mapping Spectrometer. (Bottom panel) The Gamma Ray and Neutron Detector. (Image credits, MPS/Selex Galileo/LANL)

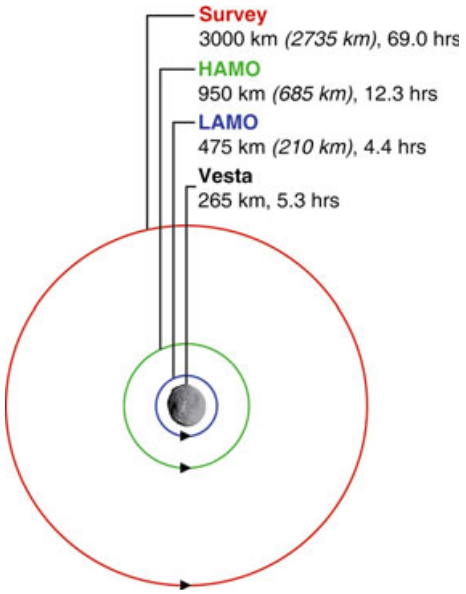

Fig. 3. The circular polar orbits used for mapping Vesta. Radial distance from center (average altitude) given in km.

Katlenburg-Lindau, with the detectors and focal plane electronics contributed by the German Aerospace Center (DLR), Institute of Planetary Research, in Berlin. The visible and infrared mapping spectrometer, or VIR, shown in Fig. 2, Panel B provides spectra over the wavelength range from 0.25 to 5 μm. It does so along a direction that can at times be orthogonal to the direction of travel and hence provide surface hyperspectral images in a "push-broom" mode, or it can scan the surface with its own mirror creating hyperspectral images (spectral cube) of a region on the surface. VIR was provided by the Institute for Space Astrophysics and Planetology, Rome and funded by ASI-Agenzia Spaziale Italiana. The third instrument shown in Fig. 2, Panel C is the Gamma Ray and Neutron Detector (GRaND) that is used to measure the elemental composition of the regolith to depths of several decimeters. GRaND was provided by the Los Alamos National Laboratory.

SCIENCE OPERATIONS

Dawn entered Vesta's gravitational sphere of influence on July 16, 2011, and exited this sphere on September 5, 2012, spending over 400 days in orbit. This period was spent in adjusting the orbit to the right altitude and viewing angle to meet the mapping requirements and for data acquisition in four orbit phases: 21 days in Survey orbit at 2735 km above the surface; 34 days in the high altitude mapping orbit 1 (HAMO1) at 685 km above the surface; 141 days in Low altitude mapping orbit (LAMO) at 210 km above

Fig. 4. Vesta and Ceres with Moon, Mercury, Mars, counter clockwise from bottom, while Vesta is found to be a much simpler body than the Moon, Mercury, and Mars, and Ceres is expected to be much simpler as well, many of the processes appearing on the larger terrestrial planets are present in primitive forms on Vesta.

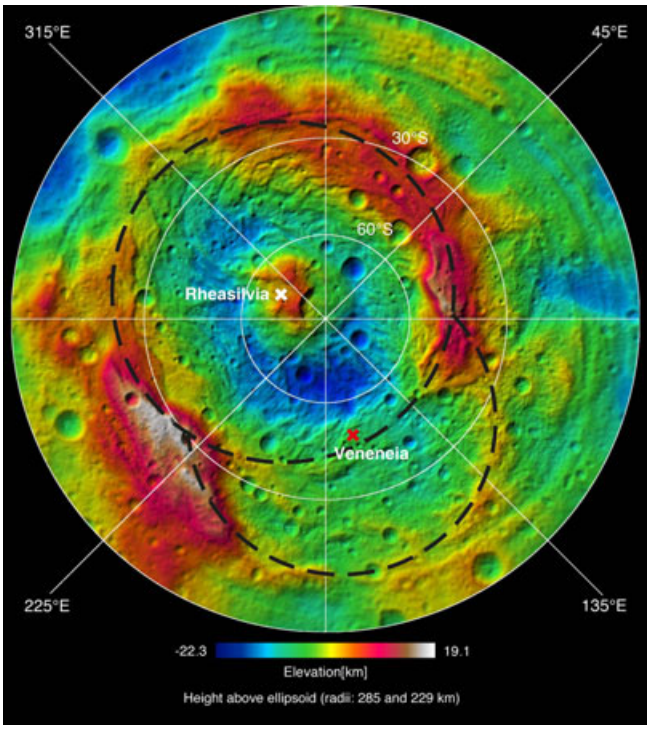

Fig. 5. Southern hemisphere survey orbit digital terrain model (DTM) with a lateral spacing of about 450 m with hill-shaded color-coded heights in polar stereographic projection (conformal). Heights are referenced to a biaxial ellipsoid, 285 × 285 × 229 km in radius. The rims of the south pole basins Rheasilvia and Veneneia are masked with dashed lines. Coordinate system in this article is that used by the Dawn team (Russell et al. 2012).

the surface; and finally 41 days in high altitude mapping orbit 2. Figure 3 shows the relative sizes of these polar orbits. During the survey orbit, the VIR instrument was the prime instrument. During HAMO1, the framing camera was the prime instrument. During LAMO, priority was given to the GRaND measurements and the gravity measurements with some data from VIR and the framing camera. While the team attempted to maximize coverage, there was no requirement for complete coverage with the framing camera or the VIR spectrometer during LAMO operations.

THE SURFACE OF VESTA

Vesta, when discovered, was thought to be a planet, but it was soon realized that Vesta and its siblings in the asteroid belt were small compared with the other planets, and they were demoted first to minor planet status, and then to asteroid status. Most recently one, and only one, Main Belt asteroid, Ceres, was promoted to dwarf planet status (IAU 2006). When compared with the Moon, Mercury, and Mars in Fig. 4, Vesta and Ceres seem very small. Nevertheless, the Dawn observations reveal that Vesta certainly has planetary characteristics (e.g., Jaumann et al. 2012). There are mountains and valleys, large graben-like tectonic systems, and craters everywhere. Factors that reduce the effect of all these impacts on Vesta include the facts that collisional velocities are smaller on Vesta because of its more distant position in the solar gravitational well, and that many of the impactors are in similar orbits.

On an absolute scale, the relief on the surface of Vesta is comparable to that seen on the Moon and Mars, about 40 km (Jaumann et al. 2012; Russell et al. 2012). In particular, the central impact mound in the Rheasilvia basin is almost the same height as the Martian Olympus Mons (the largest volcano in the solar system). When judged relative to the radius of the body, the relief on Vesta is extraordinary and is a significant factor in geologic processes.

A surprise finding was that there was not one, as known from Hubble observations (Thomas et al. 1997), but two dominant ancient basins near the south pole (Schenk et al. 2012). These two basins are shown in the topographic map derived from the digital terrain model

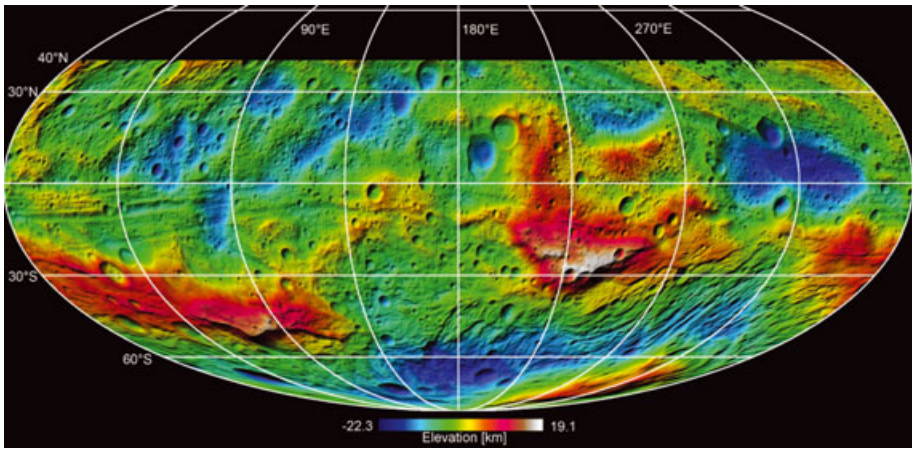

Fig. 6. Global high-altitude mapping orbit 1 (HAMO1) DTM with a lateral spacing of about 100 m with hill-shaded color-coded heights in Mollweide projection (equal-area). Heights are referenced to a biaxial ellipsoid, 285 × 285 × 229 km in radius.

in Fig. 5. These two basins have been named Rheasilvia and Veneneia. The former was created over one billion years ago and the latter well before this time (Marchi et al. 2012). These basins both have multiple rings, or more correctly troughs, surrounding them approximately halfway to their antipodal positions (Buczkowski et al. 2012a; Jaumann et al. 2012). That these huge impacts did not disrupt Vesta completely may have been in part due to the presence of Vesta's massive iron core that mitigates against fractures (Buczkowski et al. 2012b), and in part due to the lower relative velocities expected in the asteroid belt (Bottke et al. 1994).

As a result of these impacts, the regolith in the southern hemisphere is dominated by diogenite-rich ejecta, derived from the diogenite-rich lower crust/upper mantle, and the record of smaller impacts has been erased (De Sanctis et al. 2012a; Schenk et al. 2012). The equatorial region in contrast, shown in Fig. 6, is heavily cratered with mountains possibly containing ejecta from the two large basins. Crater counting shows that this "high relief terrain" is "young," but perhaps not quite as young in crater density as the Rheasilvia basin's floor (Marchi et al. 2012). At the other extreme, the most heavily cratered regions in the northern hemisphere approach 10% of the crater saturation where old craters are destroyed at the rate that new craters are created, as illustrated in Fig. 7 (Marchi et al. 2012).

Numerous unusual asymmetric impact craters and ejecta indicate the strong influence of topographic slope in cratering on Vesta. Very steep topographic slopes near to the angle of repose are common and slope failures make resurfacing, due to impacts and their associated gravitational slumping and impact-induced seismic effects, an important geologic process on Vesta (Jaumann et al. 2012).

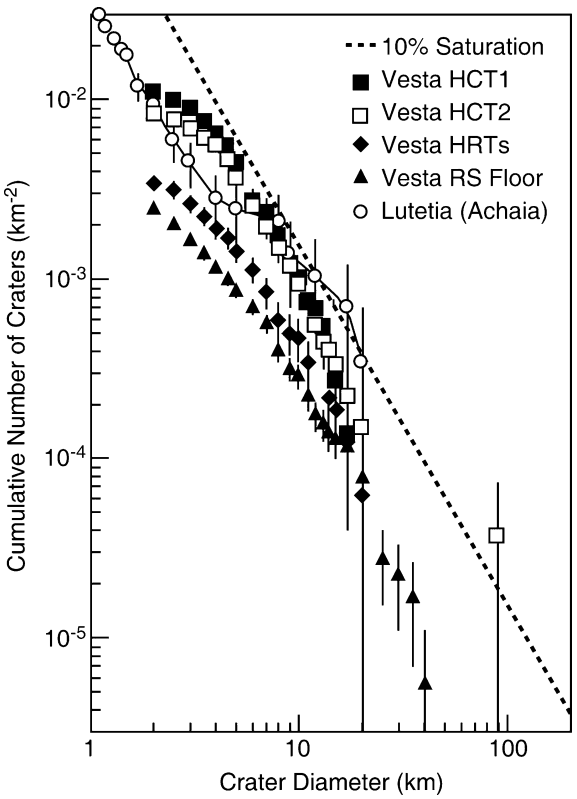

Fig. 7. Crater density versus diameter. Dashed line shows 10% of geometric saturation. HCT1 stands for heavily cratered terrain 1; HCT2 for heavily cratered terrain 2; HRT for high relief terrain; and RS for Rheasilvia (Marchi et al. 2012).

That Vesta has diverse spectral properties across its surface has been known for a long time from telescopic and Hubble Space Telescope observations (Bobrovnikoff 1929; Gaffey 1983; Binzel et al. 1997;

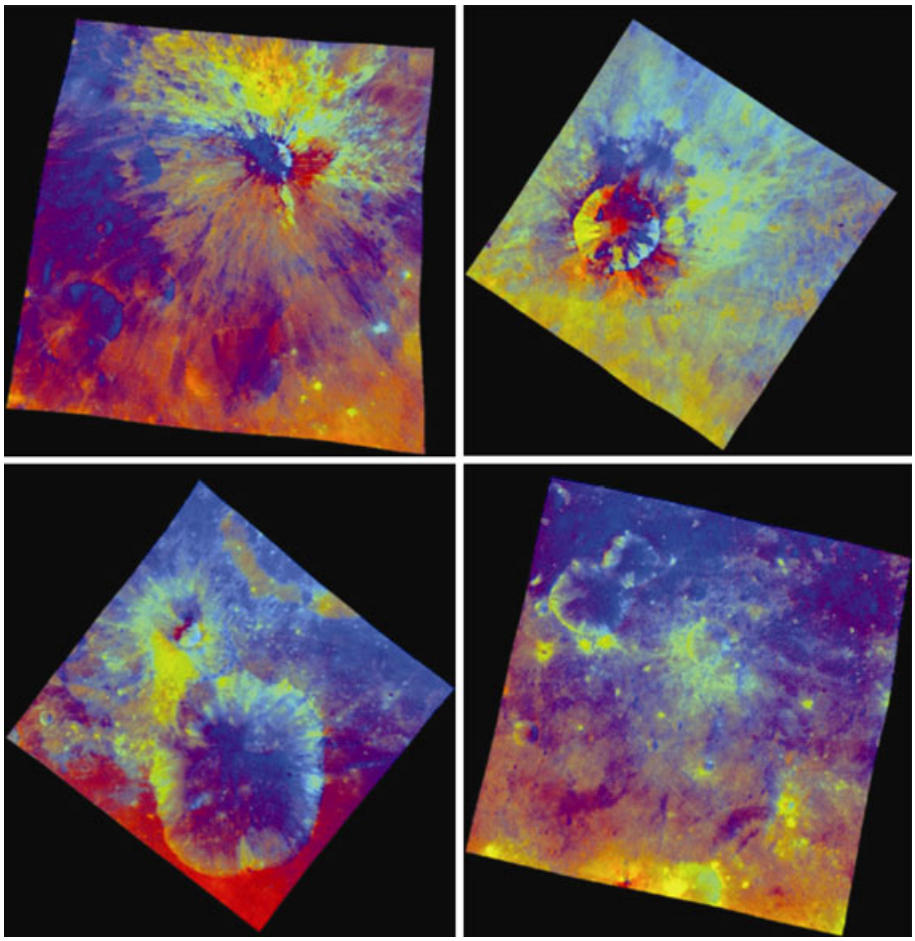

Fig. 8. Framing camera color images (similar in construction to those used for Clementine data) showing four different areas of Vesta. In this RGB color ratio R = 0.75/0.44 microns, G = 0.75/0.92, and B = 0.44/0.75 micron filters. Areas in red have red visible slope and those in blue have a bluer visible slope. Green represents areas with deeper pyroxene absorption bands. Clockwise from top left, the images show: Vibidia crater (220 °E, 26.9 °S), diameter 7.6 km; Cornelia crater (225 °E, 9.3 °S), diameter 15 km; an area (121 °E, 20.5 °S) just outside the Rheasilvia basin; Oppia crater, diameter 34 km (309 °E, 8 °S). See also Reddy et al. (2012b).

Gaffey 1997; Carry et al. 2010; Li et al. 2010; Reddy et al. 2010), but the ability to obtain high-resolution color imagery of individual craters such as those seen in Fig. 8 allows the use of color as a diagnostic tool where the shapes and locations of the colored patches give clues to the nature of the processes at work. Fresh impact craters often contain deeper absorption bands and these appear green in the color ratios of Fig. 8. For more precise characterization of the basalt identification, Dawn relies on the band depth and band center locations of pyroxene absorption around 1 and 2 μm. The presence of any other component (other minerals or molecules) is being investigated through the search of additional absorption bands and spectral variations over the entire range of wavelengths (De Sanctis et al. 2012b). As shown in Fig. 9, VIR provides an image cube of data over a broad range of wavelengths. The absorption bands shown in the lower panel are key to constraining the forms of pyroxene present and allowing mineral maps to be made.

Marcia crater (10° N, 190° E) reveals much about the nature of the near-surface crust of Vesta and the processes acting therein. Figure 10 shows the rim of Marcia, which is quite bright and shows regions of competent materials in its walls, but at some level beneath the bright layer there are patches of dark material. The excavation of Marcia cut through this patchwork of dark material and some of it spilled down the crater walls, making a striking array of black streaks on a light background. In other places, dark-rayed craters are seen suggesting that this material was transported from elsewhere in the solar system (McCord et al. 2012). This dark material appears to be an endmember of two surface components, the other endmember being bright,

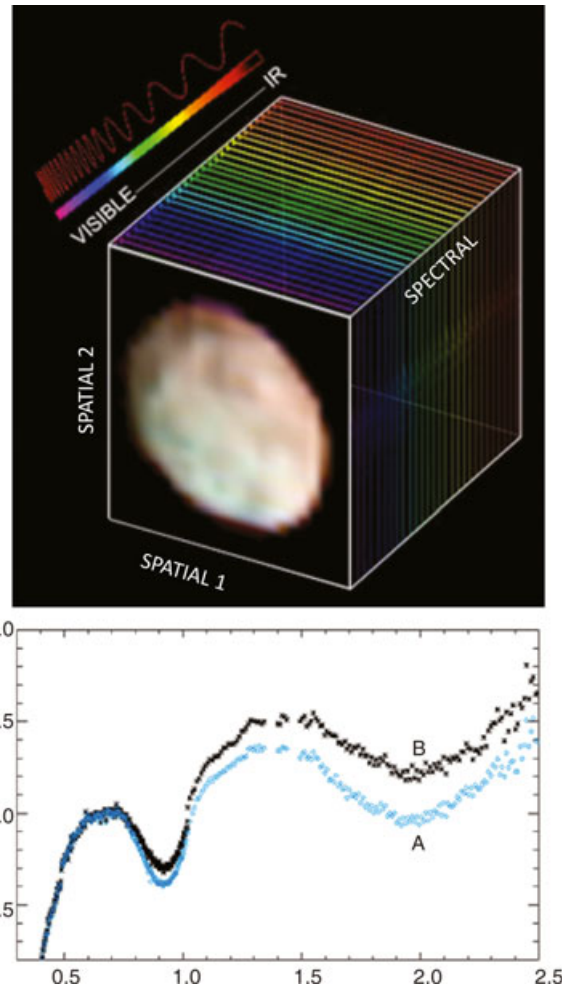

Fig. 9. (Top) The VIR spectral cube. The spectrometer obtains images at multiple wavelengths forming an image cube with two dimensions of spatial information and one dimension of spectral information. (Bottom) Each pixel includes a spectrum of a spot on the surface of Vesta, shown in De Sanctis et al. (2012a). Here, the spectra at two points A (southern hemisphere) and B (northern hemisphere) are shown. The two absorption bands evident in this figure around 1 and 2 μm are characteristic of pyroxene that constitutes the basalt of the surface. A sharp rise of the spectrum beyond 3.5 μm is due to the thermal emission. Under similar conditions of illumination, surface materials with higher reflectance at wavelengths shorter than 3.5 μm have lower thermal emission than surface materials with lower reflectance because they absorb less solar energy.

perhaps pristine, pyroxene-rich rock. Most of the surface material seems to be mixtures of these two components, both light and dark in different amounts (Jaumann et al. 2012; McCord et al. 2012). It does not take much dark material to lower the albedo of the bright material substantially. The small-scale mixing of diverse surface components appears to be the mechanism whereby the vestan surface ages (Pieters et al. 2012).

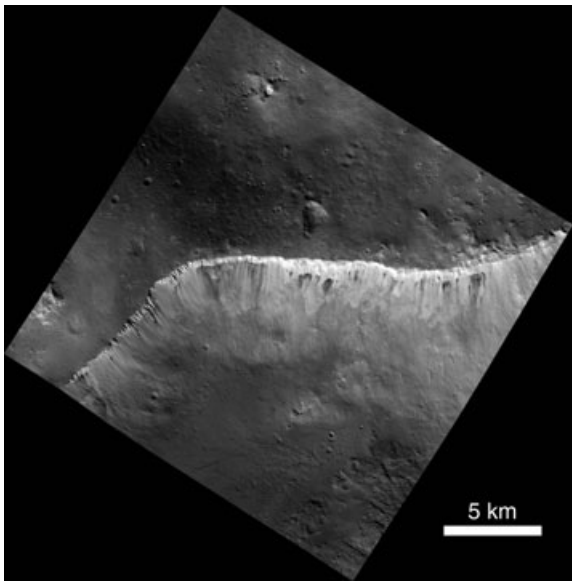

Fig. 10. The rim of Marcia crater showing the origin of dark streaks beginning at depth.

Comparison of color parameters of various meteoritical analogs suggests that carbonaceous clast-rich howardites (Buchanan et al. 1993; Zolensky et al. 1996) are the best analogs for the dark material on Vesta (McCord et al. 2012; Reddy et al. 2012). This result also confirms ground-based telescopic observations of Vesta that suggested contamination from external carbonaceous chondrites (Hasegawa et al. 2003; Rivkin et al. 2006). More recently, Reddy et al. (2012b) have proposed that the dark material came from the impactor that formed Veneneia. Nevertheless, we cannot exclude, at least partly, other sources for dark material such as impact melt or fine-grained eucritic lava.

The abundance of CM and CR carbonaceous chondrite material on the surface of Vesta estimated by Dawn FC data (<6 vol%) is consistent with HED meteorites (Zolensky et al. 1996; Herrin et al. 2011). This value is also consistent with estimates of CM-like material (<10%) proposed by Rivkin et al. (2006) and Hasegawa et al. (2003) to explain the weak 3-μm absorption feature seen by telescopic observations. VIR data confirm the presence of weak signatures in the 3 μm spectral region, interpreted as mainly due to OH (hydroxyl) near 2.8 μm (De Sanctis et al. 2012b). The 2.8 μm signatures are often associated with low-albedo areas, indicating that dark material is plausibly responsible for OH signatures. This result suggests that Vesta contains hydrated mineral phases that could have been supplied by OH-bearing impactors.

Elemental abundances measured by GRaND demonstrated that the composition of Vesta's regolith

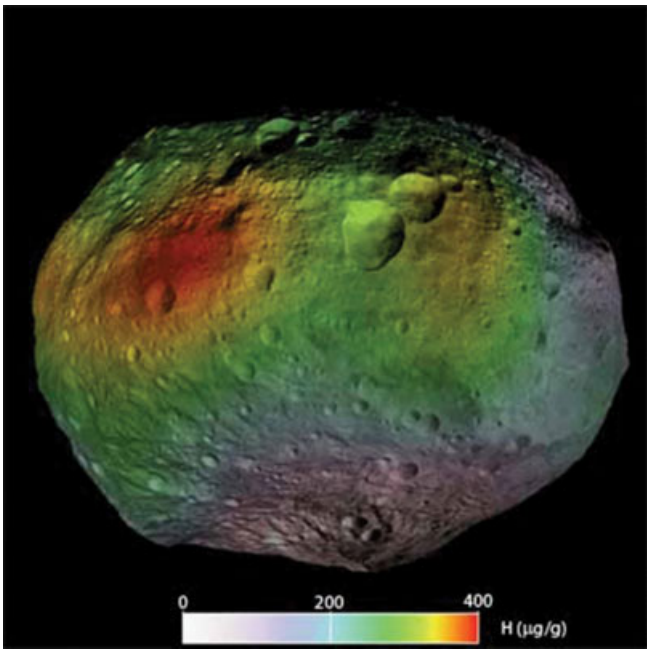

Fig. 11. Distribution of hydrogen on Vesta obtained by analysis described by Prettyman et al. (2012). Image credit T.H. Prettyman. Marcia is the bottom crater of the three adjacent craters aligned just right of center in this image. The region to the left of Marcia appears to be depleted of H relative to region farther to the west and to the east.

matches the HED meteorites; in addition, as shown in Fig. 11, GRaND globally mapped the abundance of hydrogen over the entire surface of Vesta (Prettyman et al. 2012). The highest abundances of hydrogen were found near the equator, where water ice is not stable. Very low abundances were found within the comparatively young Rheasilvia basin. Prettyman et al. (2012) also found that the abundance of hydrogen was anticorrelated with albedo. In addition, the amount of hydrogen within Vesta's regolith is consistent with that expected from carbonaceous chondrite clasts found in a few howardites. Thus, delivery of hydrous materials to Vesta was primarily by infall of carbonaceous chondrites, subject to removal, dehydration, and redistribution by impacts.

The floor of Marcia crater also shows an intriguing pitted terrain, possibly due to the delivery of volatiles incorporated within the impactor or the release of volatiles previously delivered. Figure 12 shows pits in the floor of Marcia that likely formed due to degassing of volatile-bearing material heated by the impact event (Denevi et al. 2012). The relatively low abundances of hydrogen and OH in the vicinity of Marcia (Fig. 11) may have resulted from impact-dewatering of carbonaceous materials (De Sanctis et al. 2012b; Denevi et al. 2012; Prettyman et al. 2012). The connection between Vesta, vestoids, and HED meteorites is strongly supported by near-IR spectral observations and dynamical modeling of

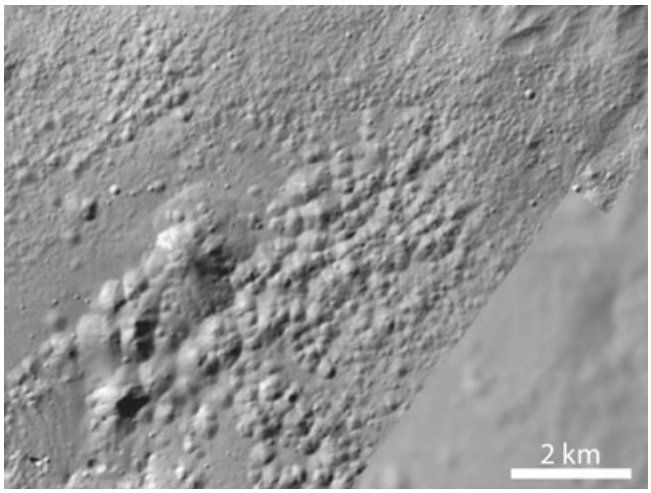

Fig. 12. Framing camera image of pitted terrain on the bottom of Marcia crater, suggesting volatiles resided within the target material discussed by Denevi et al. (2012). Image credit NASA.

the delivery mechanism (Binzel and Xu 1993). The association between hydrogen-bearing dark material on Vesta and carbonaceous chondrite clasts in howardites is yet another strong consistency with these meteorites being delivered from Vesta.

THE STRUCTURE OF THE INTERIOR

The mass of Vesta can be obtained from the period of the orbit and its volume from stereo imagery. The gravity investigation also provides the higher moments of the gravity field, most importantly the J_2 component that arises from a nonspherical core in particular. We can fit these quantities using the properties of known materials such as the meteoritic iron density, and we find that the core must be about 220 km in diameter with a crustal density similar to that of the HED. Figure 13 shows a fit to the core size and shape that returns the observed J_2 gravity term (Russell et al. 2012). The Vesta mass of 2.54×10^{20} kg is within the uncertainties of recent estimates based on observations of the motion of Mars around conjunctions with Vesta (Konopliv et al. 2011b). The size of the core is also close to that predicted from meteoritic evidence (Righter and Drake 1997; Ruzicka et al. 1997). These consistencies are important as they validate the work done prior to Dawn's observations and preserve the paradigm developed to explain Vesta as it was perceived.

THE NORTH POLE

The rotation axis of Vesta is oriented such as to keep the north pole in darkness until August 20, 2012,

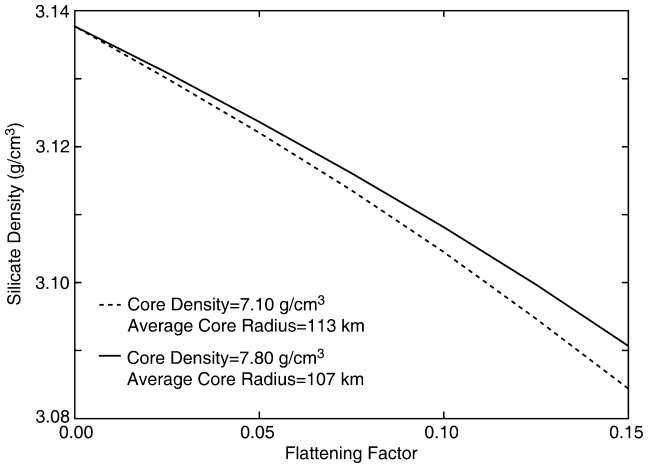

Fig. 13. Ellipsoidal cores that provide the observed J_2 gravitational moment of Vesta as a function of the silicate density of the crust (Russell et al. 2012).

only 2 weeks before Dawn escaped from Vesta's gravity field on September 5. Before August 20th, Dawn had begun to raise its orbit, resulting in lower resolution images of the surface. Moreover, even when the Sun was above the horizon near the pole, the basins and craters near the poles had shadowed floors. At the same time, the pointing of the spacecraft had to be performed on thruster control, so the net result was low-resolution, somewhat uncontrolled imagery of an incompletely lit surface. We can, however, see much of the region around the north pole, enough to gain insight into the processes at work near the antipodes of the two large impact basins. Figure 14 shows the topography returned by stereo photoclinometry using all available imagery. The northern hemisphere seems to have been little affected by the antipodal focusing of the energy from the Rheasilvia and Veneneia impacts. The study of these effects is ongoing.

LEVEL 1 OBJECTIVES

The science team developed a set of objectives for the mission that was translated into a set of measurement objectives. These objectives are kept in internal NASA documents and have not been previously published. A mission is judged to be successful when it achieves its level 1 objectives. On Dawn, our first objective was to determine the bulk density to 1%. Our second was to determine the spin axis to 0.5 degrees. The physical parameters of Vesta and its spin state are described in Table 1 (Russell et al. 2012). The accuracy obtained far exceeded that required by our level 1 objectives.

Level 1 requirement three was to determine the gravity field of Vesta to $\leq$ 90 km half-wavelength.

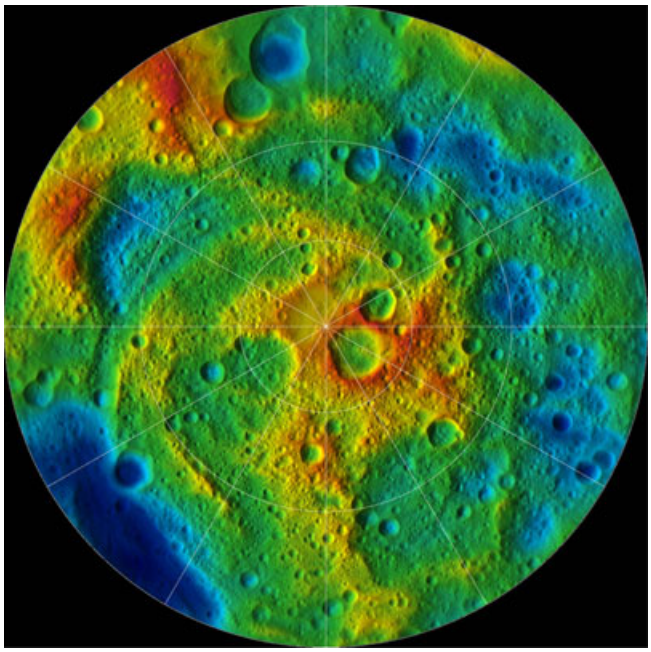

Fig. 14. Topography of the north polar regions, using Vesta shape model. Zero degrees longitude is at bottom of the figure.

Table 1. Vesta's physical parameters (Russell et al. 2012).

Volume, km^3	74.970×10^6
Mass, kg	$2.59076 \pm 0.00001 \times 10^{20}$
Bulk density, kg m^{-3}	$3456 \pm 1\%$
Gravitational flattening, J_2	$0.0317799 \pm 0.0005\%$
Spin pole R.A., deg	309.03 ± 0.01
Spin pole Dec., deg	42.24 ± 0.01
Rotation rate, deg/day	1617.333119 ± 0.000003

Figure 15 shows the gravity field of Vesta obtained from a degree and order 20 gravity model that has 45 km half-wavelength. Coherent Doppler tracking was performed using both the high-gain and low-gain antennas covering the entire body with more than 132,000 data points during LAMO.

Requirement four was to image greater than 80% of the surface of Vesta with a sampling of $\leq$100 m per pixel and a signal-to-noise ratio of at least 50 in the clear filter and in three or more color filters. The results from our HAMO-1 and HAMO-2 images are over 95% coverage in six filters and over 99% coverage in the clear filter with a spatial resolution of 60–70 m per pixel and a signal-to-noise > 100. We also obtained 66% accuracy of the surface in the LAMO orbit with a spatial resolution close to 20 m per pixel, none of which were in our requirements.

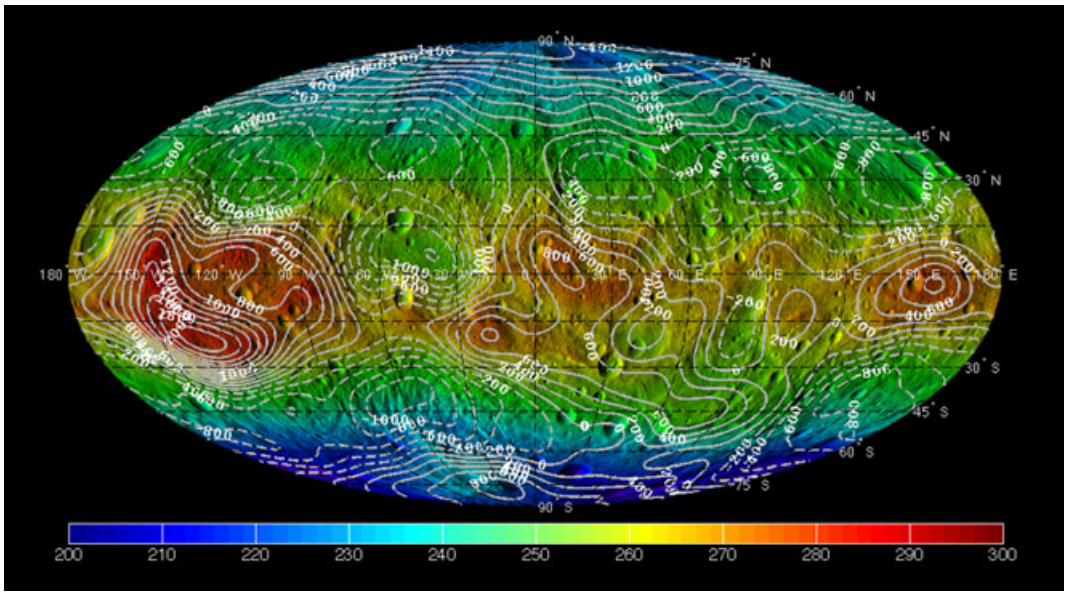

Fig. 15. Degree and order 18 gravity field calculated from LAMO data with 45 km half-wavelength resolution.

Requirement five was to obtain a topographic map of 80% of the surface with a horizontal resolution of 100 m and a vertical resolution of 10 m. Figure 6, shown earlier, illustrates the HAMO digital terrain model that has 100 m horizontal resolution and greater than 80% coverage of the surface. The height accuracy varies with the number of useable images and image quality (illumination). Coverage with at least three images that met stringent quality criteria was achieved over the entire illuminated surface. Preliminary evaluation indicates that the 3-D ray intersection error is ±7.5 m; final iterative adjustments will yield a reliable height retrieval error.

Requirement six was to measure and map the abundance of hydrogen in the top approximately 1 m of Vesta, and the abundances of rock-forming minerals to ±20%. Elemental abundances of hydrogen and iron were mapped within 15° equal-area bins, and variations with latitude and longitude were resolved. Global Fe/O Si/O (and thereby Fe/Si) were obtained with the requisite accuracy and showed agreement with the HEDs. Detection limits for *K* were determined, indicating *K* is not present. As shown by the map of neutron absorption in Fig. 11, the hydrogen mapping requirement was completed.

Requirement seven was to measure and map the mineral composition of Vesta using more than 10,000 high spectral resolution frames at wavelengths between 0.25 and 5 μm with a spectral resolution of between 2 and 10 nm. At least 5000 of these were to be at spatial resolution of better than 200 m and the rest better than 800 m. Dawn collected just shy of 50,000

Fig. 16. The visible and infrared mapping spectrometer VIR was able to obtain data over most of the planet with many fewer gaps than expected. This illustrates the coverage obtained in the HAMO-2 orbit. Image credit F. Zambon.

VIR frames at a spatial resolution <800 m that were mostly contiguous and covered nearly the entire body, and over 6800 frames at <200 m resolution. The VIR mosaic of images in Fig. 16 illustrates the excellent coverage obtained over Vesta's surface. In short, all the Vesta level 1 objectives were achieved as planned.

DISCUSSION AND CONCLUSIONS

The exploration of Vesta has revealed an object quite unlike any other planetary body. We had meteorites to tell us the geochemistry of Vesta before we had the geological context for that geochemistry—the reverse of the usual timeline of planetary exploration. Dawn has broadly confirmed inferences made from the analysis of the HED meteorites, thus strengthening the HED-Vesta connection (e.g., Keil 2002; McSween and Huss 2010). Abundance ratios for major rock-forming elements measured by GRaND are consistent with the HED paradigm that Vesta is their parent body (Prettyman et al. 2012). The geochemical analyses of the HEDs were quite informative as to what to expect at Vesta. Vesta melted and formed an iron core (Russell et al. 2012) with a crust that had lighter eucritic material on top of denser diogenitic material that we believe rests on top of an olivine-rich mantle deeper in the body (De Sanctis et al. 2012a). However, the Rheasilvia-Veneneia impacts seem not to have excavated down to an olivine-rich zone (Palomba et al. 2012), an observation that can be used to constrain conditions in the early solar system.

Vesta does not lack craters. It is nearly saturated with craters in some places. The youngest surface is in the south where the large impacts that formed Veneneia and Rheasilvia erased the earlier smaller craters (Schenk et al. 2012).

Dark, hydrous material has been delivered to the surface of Vesta by the infall of carbonaceous chondrites (McCord et al. 2012; Prettyman et al. 2012; Reddy et al. 2012a), possibly with a contribution from endogenic sources. Much of the carbonaceous material that has been brought to Vesta is incorporated into ejecta blankets or regolith through multiple cratering events. Hydrogen-rich material is widely distributed on Vesta in association with low albedo materials (De Sanctis et al. 2012b; Prettyman et al. 2012). Today we see fresh craters that have excavated through patches of dark material, forming dark streaks in crater walls. In other areas, we see dark-rayed craters possibly due to fresh dark material impacting the surface (McCord et al. 2012). The origin of a portion of the dark material is still debated. Some of the dark deposits may be endogenic, from freshly exposed mafic material or impact melt (Jaumann et al. 2012; McCord et al. 2012; Prettyman et al. 2012). However, the broad geological settings of most low-albedo material are associated with hydrogen-rich regions, consistent with the presence of OH- and H_2O-bearing phyllosilicates found in carbonaceous materials.

The occurrence of OH signature associated with dark material is further evidence of the link with hydrated material in carbonaceous chondrites. Moreover, it is clear that volatiles have played a very recent role in affecting the behavior of the surface. The pits in craters such as Marcia and Cornelia are best explained by the release of volatiles from within a melt-breccia mixture heated by the impact event (Denevi et al. 2012). These observations indicate that Vesta, and by proxy, the inner solar system, have been receiving a significant influx of primitive material from the outer asteroid belt. In conclusion, the Dawn measurements are bringing new insights to our understanding of the origin and evolution of the solar system, even as they confirm the basic tenets of our understanding of that history.

Acknowledgments—The success of the Dawn mission is due to the efforts of a large team of engineers, scientists, and administrators in industry and government laboratories both in the United States and abroad. Orbital Sciences Corporation played a major role in the development, integration, and testing of the flight system. The Dawn mission is managed by NASA's Jet Propulsion Laboratory, a division of the California Institute of Technology in Pasadena, for NASA's Science Mission Directorate, Washington DC. UCLA is responsible for overall Dawn mission science. The Dawn framing cameras have been developed and built under the leadership of the Max Planck Institute for Solar System Research, Katlenburg-Lindau, Germany, with significant contributions by DLR German Aerospace Center; Institute of Planetary Research, Berlin; and in coordination with the Institute of Computer and Communication Network Engineering, Braunschweig. The framing camera project is funded by the Max Planck Society, DLR, and NASA/JPL. The VIR visible and infrared mapping spectrometer was developed under the leadership of the Institute for Space Astrophysics and Planetology, Rome, belonging to the Italian National Institute for Astrophysics (INAF), Italy. The instrument was built by Selex-Galileo, Florence, Italy. The VIR project is funded by ASI, the Italian Space Agency, Rome. The GRaND instrument was built by Los Alamos National Laboratory and is operated by the Planetary Science Institute. Several of the co-authors are supported by NASA's Dawn at Vesta Participating Scientist program. C. T. R., H. Y. M., C. M. P., T. B. M., and J. P. C. are supported by the Discovery program through contract NNM05AA86C to the University of California, Los Angeles. A portion of this work was performed at the Jet Propulsion Laboratory, California Institute of Technology, under contract with NASA. Dawn data are archived with the NASA Planetary Data System. We thank the Dawn team for the development, cruise,

orbital insertion, and operations of the Dawn spacecraft at Vesta.

Editorial Handling—Dr. Nancy Chabot

REFERENCES

Binzel R. P. and Xu S. 1993. Chips off of asteroid 4 Vesta: Evidence for the parent body of basaltic achondrite meteorites. *Science* 260:186–191.

Binzel R. P., Gaffey M. J., Thomas P. C., Zellner B. H., Storrs A. D., and Wells E. N. 1997. Geologic mapping of Vesta from 1994 Hubble Space Telescope images. *Icarus* 128:95–103.

Bobrovnikoff N. T. 1929. The spectra of minor planets. *Lick Observatory Bulletin* 407:18–27.

Bottke W. F., Nolan M. G., Greenberg R., and Kolvoord R. A. 1994. Velocity distributions among colliding asteroids. *Icarus* 107:255–268.

Brophy J. 2011. The Dawn ion propulsion system. *Space Science Reviews* 163:251–261.

Buchanan P. C., Zolensky M. E., and Reid A. M. 1993. Carbonaceous chondrite clasts in the howardites Bholghati and EET 87513. *Meteoritics* 28:659–669.

Buczkowski D. L., Wyrick D. Y., Iyer K. A., Kahn G., Scully J. E. C., Nathues A., Gaskell R. W., Roatsch T., Preusker F., Schenk P. M., LeCorre L., Reddy V., Yingst R. A., Mest S., Williams D. A., Garry W. B., Barnouin O. S., Jaumann R., Raymond C. A., and Russell C. T. 2012a. Large-scale troughs on Vesta: A signature of planetary tectonics. *Geophysical Research Letters* 39:L18205.

Buczkowski D. L., Iyer K., Raymond C. A., Wyrick D. Y., Kahn E., Nathues A., Gaskell R. W., Roatsch T., Preusker F., and Russell C. T. 2012b. *Modeling of giant impact into a differentiated asteroid and implications for the large-scale troughs on Vesta*. San Francisco, California: AGU Meeting.

Carry B., Vernazza P., Dumas C. and Fulchignoni M. 2010. First disk-resolved spectroscopy of (4) Vesta. *Icarus* 205:473–482.

Consolmagno G. J. and Drake M. J. 1977. Composition and evolution of the eucrite parent body: Evidence from rare earth elements. *Geochimica et Cosmochimica Acta* 40: 1421–1422.

Coradini A., Turrini D., Federico C., and Magni G. 2011. Vesta and Ceres: Crossing the history of the solar system. *Space Science Reviews* 163:25–40.

De Sanctis M. C., Coradini A., Ammannito E., Filacchione G., Capria M. T., Fonte S., Magni G., Barbis A., Bini A., Dami M., Ficai-Veltroni I., Preti G., and VIR Team. 2011. The VIR spectrometer. *Space Science Reviews* 163:329–369.

De Sanctis M. C., Ammannito E., Capria M. T., Tosi F., Capaccioni F., Zambon F., Carraro F., Fonte S., Frigeri A., Jaumann R., Magni G., Marchi S., McCord T. B., McFadden L. A., McSween H. Y., Mittlefehldt D. W., Nathues A., Palomba E., Pieters C. M., Raymond C. A., Russell C. T., Toplis M. J., and Turrini D. 2012a. Spectroscopic characterization of mineralogy and its diversity across Vesta. *Science* 336:697–700.

De Sanctis M. C., Combe J.-P., Ammannito E., Palomba E., Longobardo A., McCord T. B., Marchi S., Capaccioni F., Capria M. T., Mittlefehldt D. W., Pieters C. M., Sunshine J., Tosi F., Zambon F., Carraro F., Fonte S., Frigeri A., Magni G., Raymond C. A., Russell C. T., and Turrini D. 2012b. Detection of widespread hydrated materials on Vesta by the VIR imaging spectrometer on board the Dawn mission. *The Astrophysical Journal*: 758:L36.

Denevi B. W., Blewett D. T., Buczkowski D. L., Capaccioni F., Capria M. T., DeSanctis M. C., Garry W. B., Gaskell R. W., LeCorre L., Li J.-Y., Marchi S., McCoy T. J., Nathues A., O'Brien D. P., Petro N. E., Pieters C. M., Preusker F., Raymond C. A., Reddy V., Russell C. T., Schenk P., Scully J. E. C., Sunshine J. M., Tosi F., Williams D. A., and Wyrick D. 2012. Pitted terrain on Vesta and implications for the presence of volatiles. *Science* 338:246–249.

Gaffey M. J. 1983. The asteroid 4 Vesta: Rotational spectral variations, surface material heterogeneity, and implications for origins of basaltic achondrites (abstract). 14th Lunar and Planetary Science. p. 231.

Gaffey M. J. 1997. Surface lithologic heterogeneity of asteroid 4 Vesta. *Icarus* 127:130–157.

Hasegawa S., Murakawa K., Ishiguro M., Nonaka H., Takato N., Davis C. J., Ueno M., and Hiroi T. 2003. Evidence of hydrated and/or hydroxylated minerals on the surface of Asteroid 4 Vesta. *Geophysical Research Letters* 30:2123.

Herrin J. S., Zolensky M. E., Cartwright J. A., Mittlefehldt D. W., and Ross D. K. 2011. Carbonaceous chondrite-rich howardites, the potential for hydrous lithologies on the HED parent (abstract #1608). 17th Lunar and Planetary Science Conference. CD-ROM.

IAU. 2006 General Assembly: Result of the IAU Resolution votes, accessed August 23, 2012, iau.org/public_press/news/detail/iau0603, news release, 2006.

Jaumann R., Williams D. A., Buczkowski D. L., Yingst R. A., Preusker F., Hiesinger H., Schmedemann N., Kneissl T., Vincent J. B., Blewett D. T., Buratti B. J., Carsenty U., Denevi B. W., DeSanctis M. C., Garry W. B., Keller H. U., Kersten E., Krohn K., Li J. Y., Marchi S., Matz K. D., McCord T. B., Mcsween H. Y., Mest S. C., Mittlefehldt D. W., Mottola S., Nathues A., Neukum G., O'Brien D. P., Pieters C. M., Prettyman T. H., Raymond C. A., Roatsch T., Russell C. T., Schenk P., Schmidt B. E., Scholten F., Stephan K., Sykes M. V., Tricarico P., Wagner R., Zuber M. T., and Sierks H. 2012. Vesta's shape and morphology. *Science* 336:687–690.

Keil K. 2002. Geological history of asteroid 4 Vesta: The "smallest terrestrial planet." In *Asteroids III*, edited by Bottke W. F., Cellino A., Paolicchi P., and Binzel R. P. Tucson, Arizona: University of Arizona Press. pp. 573–584.

Konopliv A. S., Asmar S. W., Bills B. G., Mastrodemos N., Park R. S., Raymond C. A., Smith D. E., and Zuber M. T. 2011a. The Dawn gravity investigation at Vesta and Ceres. *Space Science Reviews* 163:461–481.

Konopliv A. S., Asmar S. W., Folkner W. M., Karatekin O., Nunes D. C., Smrekar S. E., Yoder C. F., and Zuber M. T. 2011b. Mars high resolution gravity fields from MRO, Mars seasonal gravity, and other dynamical parameters. *Icarus* 211:401–428.

Li J.-Y., McFadden L. A., Thomas P. C., Mutchler M. J., Parker J. W., Young E. F., Russell C. T., Sykes M. V., and Schmidt B. E. 2010. Photometric mapping of asteroid (4) Vesta's southern hemisphere with Hubble Space Telescope. *Icarus* 208:238–251.

Marchi S., McSween H. Y., O'Brien D. P., Schenk P., DeSanctis M. C., Gaskell R., Jaumann R., Mottola S.,

Preusker F., Raymond C. A., Roatsch T., and Russell C. T. 2012. The violent collisional history of asteroid 4 Vesta. *Science* 336:690–694.

McCord T. B., Adams J. B., and Johnson T. V. 1970. Asteroid Vesta: Spectral reflectivity and compositional implications. *Science* 168:1445–1447.

McCord T. B., Castillo-Rogez J., and Rivkin A. 2011. Ceres: Its origin, evolution and structure and Dawn's potential contribution. *Space Science Reviews* 163:63–76.

McCord T. B., Li J.-Y., Combe J.-Ph., McSween H. Y., Jaumann R., Reddy V., Tosi F., Williams D. A., Blewett D. T., Turrini D., Palomba E., Pieters C. M., DeSanctis M. C., Ammannito E., Capria M. T., LeCorre L., Longobardo A., Nathues A., Mittlefehldt D. W., Schroeder S. E., Hiesinger H., Beck A. W., Capaccioni F., Carsenty U., Keller H. U., Denevi B. W., Sunshine J. M., Raymond C. A., and Russell C. T., and the Dawn Team. 2012. Dark material on Vesta from infall of carbonaceous volatile-rich materials. *Nature* 491: 83–86.

McFadden L. A., Wise J., Ristvey J. D. Jr., and Cobb W. 2011. The education and public outreach program for NASA's Dawn mission. *Space Science Reviews* 163:545–574.

McSween H. Y. Jr. and Huss G. R. 2010. *Cosmochemistry*. Cambridge, UK: Cambridge University Press. 568 p.

McSween H. Y. Jr., Mittlefehldt D. W., Beck A. W., Mayne R. G., and McCoy T. J. 2011. HED meteorites and their relationship to the geology of Vesta and the Dawn mission. *Space Science Reviews* 163:141–174.

O'Brien D. P. and Sykes M. V. 2011. The origin and evolution of the asteroid belt—Implications for Vesta and Ceres. *Space Science Reviews* 163:41–61.

Palomba E., De Sanctis M. C., Ammannito E., Capaccioni F., Capria M. T., Farina M., Frigeri A., Longobardo A. Tosi F., Zambon F., McSween H. Y., Mittlefehldt D. W., Russell C. T., Raymond C. A., Sunshine J., and McCord T. B. 2012. *Search for olivine spectral signatures on the surface of Vesta (Geophys. Res. Abstract 14, EGU2012-10814-1)*. Vienna, Austria: European Geophysical Union General Assembly.

Pieters C. M., McFadden L. A., Prettyman T., DeSanctis M. C., McCord T. B., Hiroi T., Klima R., Li J.-Y., and Jaumann R. 2011. Surface composition of Vesta: Issues and integrated approach. *Space Science Reviews* 163:117–139.

Pieters C. M., Ammannito E., Blewett D. T., Denevi B. W., DeSanctis M. C., Gaffey M. J., LeCorre L., Li J. Y., Marchi S., McCord T. B., McFadden L. A., Mittelfehldt D. W., Nathues A., Palmer E., Reddy V., Raymond C. A., and Russell C. T. 2012. Distinctive space weather on Vesta from regolith mixing processes. *Nature* 491:79–82.

Polanskey C. A., Joy S. P., and Raymond C. A. 2011. Dawn science planning, operations and archiving. *Space Science Reviews* 163:511–543.

Prettyman T. H., Feldman W. C., McSween H. Y. Jr., Dingler R. D., Enemark D. C., Patrick D. E., Storms S. A., Hendricks J. S., Morgenthaler J. P., Pitman K. M., and Reedy R. C. 2011. Dawn's gamma ray and neutron detector. *Space Science Reviews* 163:371–459.

Prettyman T. H., Mittlefehldt D. W., Lawrence D. J., Yamashita N., Beck A. W., Feldman W. C., McCoy T. J., McSween H. Y., Toplis M. J., Titus T. N., Tricarico P., Reedy R. C., Hendricks J. S., Forni O., LeCorre L., Li J.-Y., Mizzon H., Reddy V., Raymond C. A., and Russell C. T. 2012. Elemental mapping by Dawn reveals exogenic H in Vesta's regolith. *Science* 338:242–246.

Preusker F., Scholten F., Matz K.-D., Roatsch T., Jaumann R., Raymond C. A., and Russell C. T. 2012. Topography of Vesta from Dawn FC stereo images (EPSC abstract 2012-428-1). European Planetary Science Congress.

Raymond C. A., Jaumann R., Nathues A., Sierks H., Roatsch T., Preusker F., Scholten F., Gaskell R. W., Jorda L., Keller H.-U., Zuber M. T., Smith D. E., Mastrodemos N., and Mottola S. 2011. The Dawn topography investigation. *Space Science Reviews* 163:487–510.

Reddy V., Gaffey M. J., Kelley M. S., Nathues A., Li J.-Y., and Yarbrough R. 2010. Compositional heterogeneity of asteroid 4 Vesta's southern hemisphere: Implications for the Dawn mission. *Icarus* 210:693–706.

Reddy V., Nathues A., LeCorre L., Sierks H., Li J.-Y., Gaskell R., McCoy T., Beck A. W., Schroeder S. E., Pieters C. M., Becker K. J., Buratti B. J., Denevi B., Blewett D. T., Christensen U., Gaffey M. J., Gutierrez-Marques P., Hicks M., Keller H. U., Maue T., Mottola S., McFadden L. A., McSween H. Y., Mittlefehldt D., O'Brien D. P., Raymond C., and Russell C. T. 2012a. Color and albedo heterogeneity of Vesta from Dawn. *Science* 336:700–704.

Reddy V., LeCorre L., Nathues A., O'Brien D. P., Cloutis E. A., Durda D. D., Bottke W. F., Bhatt M. U., Nesvorny D., Buczkowski D., Scully J. E. C., Palmer E. M., Sierks H., Mann P. J., Becker K. J., Beck A. W., Mittlefehldt A., Li J.-Y., Gaskell R., Russell C. T., Gaffey M. J., McSween H. Y., McCord T. B., Combe J.-P., and Blewett D. 2012b. Delivery of dark material to Vesta via carbonaceous chondritic impacts. *Icarus* 221:544–559.

Righter K. and Drake M. J. 1997. A magma ocean on Vesta: Core formation and petrogenesis of eucrites and diogenites. *Meteoritics & Planetary Science* 32:929–944.

Rivkin S., McFadden L. A., Binzel R. P., and Sykes M. 2006. Rotationally-resolved spectroscopy of Vesta I: 2-4 um region. *Icarus* 180:464–472.

Rivkin A.S., Li J.-Y., Milliken R. E., Lim L. F., Lovell A. J., Schmidt B. E., McFadden L. A., and Cohen B. A. 2011. The surface composition of Ceres. *Space Science Reviews* 163:95–116.

Russell C. T. and Raymond C.A. 2011. The Dawn Mission to Vesta and Ceres. *Space Science Reviews* 163:3–23.

Russell C. T., Raymond C. A., Coradini A., McSween H. Y., Zuber M. T., Nathues A., De Sanctis M. C., Jaumann R., Konopliv A. S., Preusker F., Asmar S. W., Park R. S., Gaskell R., Keller H. U., Mottola S., Roatsch T., Scully J. E. C., Smith D. E., Tricarico P., Toplis M. J., Christensen U. R., Feldman W. C., Lawrence D. J., McCoy T. J., Prettyman T. H., Reedy R. C., Sykes M. E., and Titus T. N. 2012. Dawn at Vesta: Testing the protoplanetary paradigm. *Science* 336:684–686.

Ruzicka A., Snyder G. A., and Taylor L. A. 1997. Vesta as the howardite, eucrite, and diogenite parent body: Implications for the size of a core and for large-scale differentiation. *Meteoritics & Planetary Science* 32:825–840.

Schenk P., O'Brien D. P., Marchi S., Gaskell R., Preusker F., Roatsch T., Jaumann R., Buczkowski D., McCord T., McSween H. Y., Williams D., Yingst A., Raymond C., and Russell C. T. 2012. The geologically recent giant impact basins at Vesta's south pole. *Science* 336:694–697.

Sierks H., Keller H. U., Jaumann R., Michalik H., Behnke T., Bubenhagen F., Buttner I., Carsenty U., Christensen U., Enge R., Fiethe B., Gutierrez-Marques P., Hartwig H., Kruger H., Kuhne W., Maue T., Mottola S., Nathues A., Reiche K.-U., Richards M. L., Roatsch T.,

Schroeder S. E., Szemerey I., and Tschentscher M. 2011. The Dawn framing camera. *Space Science Reviews* 163:263–327.

Thomas P. C., Binzel R. P., Gaffey M. J., Zellner B. H., Storrs A. D., and Wells E. 1997. Vesta: Spin pole, size, shape from HST images. *Icarus* 128:88–94.

Thomas V. C., Makowski J. M., Mark Brown G., McCarthy J. F., Bruno D., Christopher Cardoso J., Michael Chiville W., Meyer T. F., Nelson K. E., Pavri B. E., Termohlen D. A., Violet M. D., and Williams J. B. 2011. The Dawn spacecraft. *Space Science Reviews* 163:175–249.

Zolensky M. E., Weisberg M. K., Buchanan P. C., and Mittlefehldt D. W. 1996. Mineralogy of carbonaceous chondrite clasts in HED achondrites and the Moon. *Meteoritics* 31:518–537.

Zuber M. T., McSween H. Y. Jr., Binzel R. P., Elkins-Tanton L. T., Konopliv A. S., Pieters C. M., and Smith D. E. 2011. Origin, internal structure and evolution of 4 Vesta. *Space Science Reviews* 163:77–93.